Hindawi
Mathematical Problems in Engineering
Volume 2019, Article ID 4507852, 12 pages
https://doi.org/10.1155/2019/4507852

Research Article

Magnetohydrodynamic (MHD) Boundary Layer Flow Past a Wedge with Heat Transfer and Viscous Effects of Nanofluid Embedded in Porous Media

Wubshet Ibrahim[1] **and Ayele Tulu**[2]

[1]*Department of Mathematics, Ambo University, Ambo, Ethiopia*
[2]*Department of Mathematics, Wollega University, Nekete, Ethiopia*

Correspondence should be addressed to Wubshet Ibrahim; wubshetib@yahoo.com

Received 10 November 2018; Revised 31 December 2018; Accepted 13 January 2019; Published 30 January 2019

Academic Editor: Hang Xu

The problem of two-dimensional steady laminar MHD boundary layer flow past a wedge with heat and mass transfer of nanofluid embedded in porous media with viscous dissipation, Brownian motion, and thermophoresis effect is considered. Using suitable similarity transformations, the governing partial differential equations have been transformed to nonlinear higher-order ordinary differential equations. The transmuted model is shown to be controlled by a number of thermophysical parameters, viz. the pressure gradient, magnetic, permeability, Prandtl number, Lewis number, Brownian motion, thermophoresis, and Eckert number. The problem is then solved numerically using spectral quasilinearization method (SQLM). The accuracy of the method is checked against the previously published results and an excellent agreement has been obtained. The velocity boundary layer thickness reduces with an increase in pressure gradient, permeability, and magnetic parameters, whereas thermal boundary layer thickness increases with an increase in Eckert number, Brownian motion, and thermophoresis parameters. Greater values of Prandtl number, Lewis number, Brownian motion, and magnetic parameter reduce the nanoparticles concentration boundary layer.

1. Introduction

Fluid flows with convective heat and mass transfer over a wedge shaped bodies is ensured in many thermal engineering applications like crude oil extraction, geothermal systems, thermal insulation, heat exchangers, and the storage of nuclear waste, Nagendramma et al. [1]. A model of steady laminar fluid flow over a wedge has developed for the first time by Falkner and Skan [2] to illustrate the application of Prandtl's boundary layer theory. Late, Hartree [3] investigated the same problem with similarity transformation and gave numerical results for wall shear stress for different values of the wedge angle. Eckert [4] also solved Falkner-Skan flow along an isothermal wedge and presented the first wall heat transfer values. Afterward, the variety of applications and understanding of the physical features of laminar boundary layer flow past a wedge have motivated many researchers (to mention a few, Martin and Boyd [5], Sattar [6], Kandasamy et al [7], and Turkyilmazoglu [8]).

Magnetohydrodynamic (MHD) is the study of fluid flow in electrically conducting fluids with magnetic properties that affect fluid flow characteristics. When a magnetic field is incident in an electrically conducting fluid, a current is induced. This effect polarizes the fluid and as a result the magnetic field is changed (Makanda et al. [9]). Due to extensive practical applications of MHD in technological processes such as plasma studies, petroleum industries, MHD power generator designs, design for cooling of nuclear reactors, and construction of heat exchangers and on the performance of many other systems, there are many studies that considered MHD fluid flow past a wedge. These include the work of Abbasbandy et al. [10] who examined the effects of MHD in the Falken-Skan flow of Maxwell fluid, and El-Dabe et al. [11] considered the MHD boundary layer flow of non-Newtonian

Casson fluid on a moving wedge with heat and mass transfer. Khan et al. [12] also analyzed MHD laminar boundary layer flow past a wedge with the influence of thermal radiation, heat generation, and chemical reaction.

In the past few years, MHD boundary layer flow with heat and mass transfer of nanofluids has become a major topic of modern-day interest. Nanofluids have a significant role in enhancing the heat transfer properties of fluids. The most important properties of nanofluids are enhanced effective fluid thermal conductivity and heat transfer coefficient. Some recent studies on MHD boundary layer flow of nanofluid include the work of the Srinivasacharya et al. [13] who analyzed the steady laminar MHD flow in a nanofluid over a wedge in the presence of a variable magnetic field. Rasheed et al. [14] also investigated MHD boundary layer flow of nanofluid over a continuously moving stretching surface. The effects of thermal radiation on mixed convection flow of nanofluid over a stretching sheet in the presence of a magnetic field are studied by Nageeb et al. [15].

Viscous dissipation effect changes the temperature distribution by playing a role like an energy source, which leads to affected heat transfer rate and hence needs to be considered in heat transfer problems. The analysis of MHD boundary layer flows in porous media with and without the effect of viscous dissipation has been a subject of several recent researchers. Accordingly, Arthur et al. [16] analyzed hydromagnetic stagnation point flow over a porous stretching surface in the presence of thermal radiation and viscous dissipation effects. Also, Ramesh et al. [17] studied the MHD boundary layer flow past a constant wedge within porous media. Heat and mass transfer of MHD flow of nanofluids in the presence of viscous dissipation effects are numerically analyzed by Haile and Shankar [18]. Majety et al. [19] studied the effect of viscous dissipation on MHD boundary layer flow past a wedge through porous medium. They concluded that viscous dissipation produces heat due to drag between the fluid particles, which cause an increase in fluid temperature.

Most of the standard methods of solving the boundary layer problems are the numerical approach based on the shooting algorithm with the Runge-Kutta scheme, finite difference method, spectral homotopy analysis method, and Newton-Raphson based methods such as the quasilinearization method and the successive linearization method. Recently, spectral based numerical techniques such as the Spectral Quasilinearization Method and Spectral Relaxation Method have been developed (see Motsa et al. [23], Motsa [24], and Magagula et al. [25]). As indicated by Motsa et al. [26] and Zhou [27] Chebyshev spectral collocation methods are easy to implement and adaptable to various problems and provide more accurate approximations with a relatively small number of unknowns. Gottlieb and Hesthaven [28] also added that the wide use of spectral methods has motivated the researcher by their accuracy and efficiency in solving incompressible Navier-Stokes equations. Furthermore, Motsa et al. [29] stated that the interest in using Chebyshev spectral collocation methods in solving nonlinear PDEs stems from the fact that these methods require less grid points to achieve accurate results and efficient compared to traditional methods like finite difference and finite element methods.

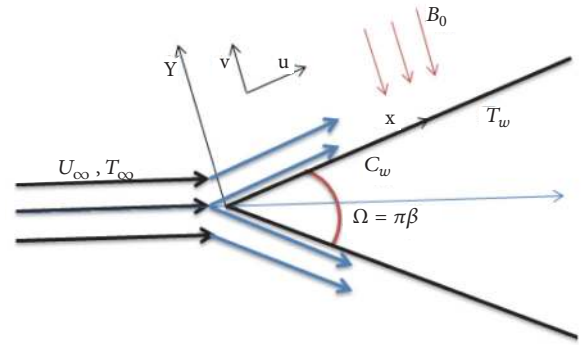

Figure 1: Physical model of flow configuration and coordinate system.

The present study deals with MHD boundary layer flow past a wedge with heat and mass transfer of nanofluid embedded in a porous media with viscous dissipation, Brownian motion, and thermophoresis parameter effects. Using appropriate similarity transformation, the governing nonlinear partial differential equations are transformed to nonlinear higher-order ordinary differential equations. Then, these equations are numerically solved using Spectral Quasilinearization Method. The effects of different parameters on velocity, temperature, and concentration fields are investigated and analyzed with the help of their graphical and tabular representations.

2. Mathematical Formulation

Consider steady two-dimensional, laminar boundary layer flow past a wedge with heat transfer of incompressible electrically conducting nanofluid embedded in a porous media with viscous dissipation effects. The coordinate system is chosen with x coordinate pointing parallel to the plate in the direction of the flow and y coordinate pointing towards the free stream, as shown in the Figure 1. The wall of the wedge is maintained with uniform and constant temperature T_w and nanoparticle concentration C_w. T_w and C_w are, respectively, greater than the ambient temperature T_∞ and ambient nanoparticle concentration C_∞. The subscripts w and ∞ denote conditions at wall and ambient, respectively. The fluid is assumed to have constant physical properties.

It is also assumed that a constant magnetic field B_0 is applied in the positive y-direction, normal to the walls of the wedge. The induced magnetic field caused by the motion of electrically conducting fluid is neglected, as it is very small compared to applied magnetic field (Ullah et al. [22]). The Naiver-Stokes equation of motion including electromagnetic body force or Lorentz force within conductive media is given by $F = J_c \times B$, where J_c is the conduction current defined as $J_c = \sigma(E + \mathbf{u} \times B)$, B is the magnetic field, E is the electric field, $\mathbf{u}$ is the velocity vector of the fluid, and σ is the electrical conductivity of the fluid (Nicholas [30]). Since the induced magnetic field caused by the motion of electrically conducting fluid E is negligible as compared to the applied

magnetic field B, then $J_c = \sigma(\mathbf{u}\times B) = \sigma[(u, v, 0)\times 0, B_y, 0)] = \sigma u B_y \hat{k}$. Thus, the Lorentz force $F = J_c \times B = (0, 0, \sigma u B_y) \times (0, B_y, 0) = -\sigma B_y^2 u\hat{i} = -\sigma B_0^2 u$.

We use the general model of the conservation equation for a general scalar variable φ which can be expressed as (see Versteeg and Malalasekera [31])

$$\frac{\partial(\rho\varphi)}{\partial t} + \nabla.(\rho\mathbf{u}\varphi) = \nabla.(\Gamma\nabla\varphi) + S_\varphi \tag{1}$$

where the velocity vector given by $\mathbf{u} = \langle u, v, w\rangle$, ρ is density of the fluid, Γ is the diffusion coefficient, and S_φ is the source term. Equation (1) is the so-called transport equation for property φ, and it clearly highlights the various transport processes.

By setting φ equal to 1, $\mathbf{u}$, temperature of fluid T, and nanoparticle concentration C in (1) and selecting appropriate values for diffusion coefficient Γ and source terms S_φ, we obtain special forms of PDEs (Navier-Stokes equations) for the continuity, momentum, energy, and nanoparticle concentration. With the above assumptions and the boundary layer approximations, the continuity, momentum, energy, and nanoparticle concentration equations governing steady two-dimensional MHD boundary layer flow past a wedge embedded in a porous media with viscous dissipation effects and constant fluid properties are given as (see Srinivasacharya et al. [13], Haile and Shankar [18], and Alam et al. [32]).

$$\frac{\partial u}{\partial x} + \frac{\partial v}{\partial y} = 0 \tag{2}$$

$$u\frac{\partial u}{\partial x} + v\frac{\partial u}{\partial y} = -\frac{1}{\rho_f}\frac{\partial p}{\partial x} + \nu_f\frac{\partial^2 u}{\partial y^2} - \left(\frac{\sigma B_0^2}{\rho_f} + \frac{\nu_f}{K}\right)u \tag{3}$$

$$u\frac{\partial T}{\partial x} + v\frac{\partial T}{\partial y} = \alpha_f\frac{\partial^2 T}{\partial y^2} + \frac{\nu_f}{C_p}\left(\frac{\partial u}{\partial y}\right)^2 + \tau\left\{D_B\left(\frac{\partial T}{\partial y}\frac{\partial C}{\partial y}\right) + \frac{D_T}{T_\infty}\left(\frac{\partial T}{\partial y}\right)^2\right\} \tag{4}$$

$$u\frac{\partial C}{\partial x} + v\frac{\partial C}{\partial y} = D_B\frac{\partial^2 C}{\partial y^2} + \frac{D_T}{T_\infty}\frac{\partial^2 T}{\partial y^2} \tag{5}$$

The appropriate boundary conditions are given as

$$\begin{aligned} &u = 0;\\ &v = 0;\\ &T = T_w;\\ &C = C_w, \end{aligned} \qquad \text{at } y = 0 \tag{6}$$

$$\begin{aligned} &u = U(x) = U_\infty x^m;\\ &T \longrightarrow T_\infty;\\ &C \longrightarrow C_\infty, \end{aligned} \qquad \text{as } y \longrightarrow \infty \tag{7}$$

$$\begin{aligned} &u = U_\infty;\\ &T = T_\infty, \end{aligned} \qquad at\ x = 0 \tag{8}$$

where u and v are, respectively, the x and y velocity components. ρ_f, ν_f, α_f, and C_p, are respectively, density, kinematic viscosity, thermal diffusivity, and specific heat capacity of the base fluid. K is the permeability of porous medium, D_B is the Brownian diffusion coefficient, D_T is the thermophoresis diffusion coefficient, and τ is the ratio of the effective heat capacity of the nanoparticle material and the heat capacity of base fluid.

The y-momentum equation implies that the pressure p in the boundary layer must be equal to that of the free stream for any given x coordinate. Because the velocity profile is uniform in the free stream, there is no vorticity involved; therefore, simple Bernoulli's equation can be applied in this high Reynolds number (Falkner and Skan [2]). It is assumed that $U(x) = U_\infty x^m$ is the fluid velocity at the wedge outside the boundary layer, where U_∞ is the free stream velocity. For a uniform stream, the momentum equation (3) becomes (see Falkner and Skan [2], and Nageeb et al. [15])

$$-\frac{1}{\rho_f}\frac{\partial p}{\partial x} = U\frac{dU}{dx} + \left(\frac{\sigma B_0^2}{\rho_f} + \frac{\nu_f}{K}\right)U \tag{9}$$

Substituting (9) into (3), the momentum equation is written as

$$u\frac{\partial u}{\partial x} + v\frac{\partial u}{\partial y} = U\frac{dU}{dx} + \nu_f\frac{\partial^2 u}{\partial y^2} + \left(\frac{\sigma B_0^2}{\rho_f} + \frac{\nu_f}{K}\right)(U - u) \tag{10}$$

Here, x is measured from the tip of the wedge, m is the Falkner-Skan power-law parameter, and $\beta = 2m/(1 + m)$ is the Hartree pressure gradient parameter corresponding to $\beta = \Omega/\pi$ for the total angle Ω of the wedge (see Figure 1). Physically, $m < 0$ corresponding to an adverse pressure gradient (often resulting in boundary layer separation) while $m > 0$ represents favorable pressure gradient (Nagendramma et al. [1]). In the Blasius solution $m = 0$ corresponding to an angle of attack of zero radians, where $m = 1$ corresponding to stagnation point flow.

In order to transform the governing equations (2)-(7) to a set of ordinary differential equations, introduce the stream function $\psi(x, y)$ such that

$$u = \frac{\partial \psi}{\partial y}$$
$$v = -\frac{\partial \psi}{\partial x} \tag{11}$$

and we use the following transformation variables (see Ullah et al. [22], and Alam et al. [32]):

$$\eta = y\sqrt{\frac{1+m}{2}\frac{U_\infty}{\nu_f}}x^{(m-1)/2};$$
$$\psi(x,\eta) = \sqrt{\frac{2}{1+m}\nu_f U_\infty}x^{(m+1)/2} f(\eta)$$
$$f'(\eta) = \frac{u}{U}; \tag{12}$$
$$\theta(\eta) = \frac{T - T_\infty}{T_w - T_\infty};$$
$$\phi(\eta) = \frac{C - C_\infty}{C_w - C_\infty}$$

where η is a dimensionless similarity variable, $f(\eta)$ nondimensional stream function, $f'(\eta)$ is non-dimensional velocity, $\theta(\eta)$ is nondimensional temperature, and $\phi(\eta)$ is nondimensional nanoparticle concentration.

Upon substituting similarity variables into (3)-(7), the continuity equation (2) is identically satisfied and the following system of ordinary differential equations is obtained:

$$f''' + ff'' + \beta\left[1 - f'^2\right] + \frac{1}{1+m}(M+\kappa)\left[1 - f'\right] = 0 \tag{13}$$

$$\theta'' + Pr\left[f\theta' + Ecf''^2 + Nb\theta'\phi' + Nt\theta'^2\right] = 0 \tag{14}$$

$$\phi'' + LePr\left(f\phi'\right) + \frac{Nt}{Nb}\theta'' = 0 \tag{15}$$

The transformed boundary conditions are

$$f = 0;$$
$$f' = 0;$$
$$\theta = 1; \tag{16}$$
$$\phi = 1,$$
$$at\ \eta = 0;$$
$$f' \longrightarrow 1;$$
$$\theta \longrightarrow 0; \tag{17}$$
$$\phi \longrightarrow 0,$$
$$as\ \eta \longrightarrow \infty$$

with

$$M = \frac{2\sigma B_0^2 x^{1-m}}{\rho_f U_\infty};$$
$$\kappa = \frac{2\nu_f x^{1-m}}{KU_\infty};$$
$$Ec = \frac{U^2}{C_p(T_w - T_\infty)};$$
$$Pr = \frac{\nu_f}{\alpha_f}$$
$$Le = \frac{\alpha_f}{D_B}; \tag{18}$$
$$Nb = \frac{\tau D_B(C_w - C_\infty)}{\nu_f};$$
$$Nt = \frac{\tau D_T(T_w - T_\infty)}{\nu_f T_\infty};$$
$$\mathrm{Re}_x = \frac{U_w x}{\nu_f}$$

where M is magnetic parameter, Re_x is local Reynolds number, Pr is Prandtl number, Ec is Eckert number, κ is the permeability parameter, Le is Lewis number, Nb is the Brownian motion parameter, Nt is the thermophoretic parameter, and prime ($'$) denotes derivative with respect to η.

The physical quantities of engineering interest in the present study are the skin friction coefficient C_f, local Nusselt number Nu_x, and local Sherwood number Sh_x, respectively, and defined as

$$C_f = \frac{2\tau_w}{\rho U^2(x)};$$
$$Nu_x = \frac{xq_w}{k(T_w - T_\infty)}; \tag{19}$$
$$Sh_x = \frac{xM_w}{D_B(C_w - C_\infty)};$$

where τ_w, q_w, and M_w are the surface shear stress, the surface heat flux, and surface mass flux; and, respectively, they are given as

$$\tau_w = \mu_f\left(\frac{\partial u}{\partial y}\right)_{y=0};$$
$$q_w = -k_f\left(\frac{\partial T}{\partial y}\right)_{y=0}; \tag{20}$$
$$M_w = -D_B\left(\frac{\partial C}{\partial y}\right)_{y=0}$$

The nondimensional skin friction coefficient, local Nusselt number, and local Sherwood number are, respectively, given as

$$C_f\sqrt{\mathrm{Re}_x} = 2\sqrt{\frac{m+1}{2}}f''(0);$$
$$\frac{Nu_x}{\sqrt{\mathrm{Re}_x}} = -\sqrt{\frac{m+1}{2}}\theta'(0); \quad (21)$$
$$\frac{Sh_x}{\sqrt{\mathrm{Re}_x}} = -\sqrt{\frac{m+1}{2}}\phi'(0)$$

3. Numerical Method

The system of nonlinear ODE (13)-(15) subjected to the boundary conditions (17) has been solved numerically using spectral quasilinearization method (SQLM). The main idea behind this method is identifying univariate and multivariate nonlinear terms of function and its derivative in each of the equations of the systems (13)-(15), linearizing the terms and applying Chebychev pseudospectral collocation method (see Motsa [33]).

Applying spectral quasilinearization method, (13)-(15) give the following iterative sequence of linear differential equations:

$$f'''_{r+1} + a_{1,r}f''_{r+1} - a_{2,r}f'_{r+1} + a_{3,r}f_{r+1} = a_{4,r} \quad (22)$$
$$\theta''_{r+1} + b_{1,r}\theta'_{r+1} + b_{2,r}f''_{r+1} + b_{3,r}f_{r+1} + b_{4,r}\phi'_{r+1} = b_{5,r} \quad (23)$$
$$\phi''_{r+1} + c_{1,r}\phi'_{r+1} + c_{2,r}f''_{r+1} + c_{3,r}f_{r+1} + c_{4,r}\theta'_{r+1} = c_{5,r} \quad (24)$$

where the terms containing $r+1$ subscripts denote current approximations and terms containing r subscripts denote previous approximations. The corresponding boundary conditions are

$$f_{r+1}(0) = 0;$$
$$f'_{r+1}(0) = 0, \quad (25)$$
$$f'_{r+1}(\infty) \longrightarrow 1$$
$$\theta_{r+1}(0) = \phi_{r+1}(0) = 1,$$
$$\theta_{r+1}(\infty) = \phi_{r+1}(\infty) \longrightarrow 0 \quad (26)$$

where

$$a_{1,r} = f_r;$$
$$a_{2,r} = 2\beta f'_r + \frac{1}{1+m}(M+\kappa);$$
$$a_{3,r} = f''_r;$$
$$a_{4,r} = f_r f''_r - \beta\left(1 + f'^2_r\right) - \frac{1}{1+m}(M+\kappa)$$
$$b_{1,r} = Pr\left(f_r + Nb\phi'_r + 2Nt\theta'_r\right);$$
$$b_{2,r} = 2PrEcf''_r;$$
$$b_{3,r} = Pr\theta'_r;$$
$$b_{4,r} = PrNb\theta'_r$$
$$b_{5,r} = PrEcf''^2_r + PrNb\theta'_r\phi'_r + PrNt\theta'^2_r + Prf_r\theta'_r;$$
$$c_{1,r} = Pr\left(Lef_r - Nt\theta'_r\right)$$
$$c_{3,r} = Pr\left(Le\phi'_r - \left(\frac{Nt}{Nb}\right)\theta'_r\right);$$
$$c_{4,r} = -Pr\left(\frac{Nt}{Nb}\right)\left(f_r + Nb\phi'_r + 2Nt\theta'_r\right)$$
$$c_{2,r} = -2PrEc\left(\frac{Nt}{Nb}\right)f''_r;$$
$$c_{5,r} = Pr\left\{Lef_r\phi'_r - \left(\frac{Nt}{Nb}\right)\left[Ecf''^2_r + Nb\theta'_r\phi'_r + Nt\theta'^2_r + f_r\theta'_r\right]\right\} \quad (27)$$

The physical domain on which the system of governing equations (13)-(15) defined in $[0,\infty)$ is moved to $[-1,1]$ using the transformation $x = 2\eta/L_\infty - 1$, where L_∞ is a scaling parameter assumed to be large and the interval $[0,\infty)$ is replaced by $[0, L_\infty]$. Spectral collocation method is applied to the system of (22)-(24); and the differentiation matrix $\mathbf{D} = 2D/L_\infty$ is used to approximate derivatives of unknown variables, where D is $(N+1)\times(N+1)$ Chebyshev differentiation matrix (see Trefethen [34]). The system of (22)-(24) is solved as a coupled matrix:

$$\begin{bmatrix}\Lambda_{11} & \Lambda_{12} & \Lambda_{13}\\ \Lambda_{21} & \Lambda_{22} & \Lambda_{23}\\ \Lambda_{31} & \Lambda_{32} & \Lambda_{33}\end{bmatrix}\begin{bmatrix}F_{r+1}\\ \Theta_{r+1}\\ \Phi_{r+1}\end{bmatrix} = \begin{bmatrix}R_1\\ R_2\\ R_3\end{bmatrix} \quad (28)$$

with transformed boundary condition

$$F_{r+1}\left(x_{N_x}\right) = 0,$$
$$F_{r+1}\left(x_{N_x-1}\right) = 0, \quad (29)$$
$$F_{r+1}\left(x_0\right) = 1$$
$$\Theta_{r+1}\left(x_{N_x}\right) = 1,$$
$$\Theta_{r+1}\left(x_0\right) = 0; \quad (30)$$
$$\Phi_{r+1}\left(x_{N_x}\right) = 1,$$
$$\Phi_{r+1}\left(x_0\right) = 0$$

where

$$
\begin{aligned}
R_1 &= a_{4,r};\\
R_2 &= b_{5,r};\\
R_3 &= c_{5,r}\\
\Lambda_{11} &= \mathbf{D}^3 + \operatorname{diag}(a_{1,r})\,\mathbf{D}^2 - \operatorname{diag}(a_{2,r})\,\mathbf{D}\\
&\quad + \operatorname{diag}(a_{3,r});\\
\Lambda_{12} &= \mathbf{O};\\
\Lambda_{13} &= \mathbf{O}\\
\Lambda_{21} &= \operatorname{diag}(b_{2,r})\,\mathbf{D}^2 + \operatorname{diag}(b_{3,r});\\
\Lambda_{22} &= \mathbf{D}^2 + \operatorname{diag}(b_{1,r})\,\mathbf{D};\\
\Lambda_{23} &= \operatorname{diag}(b_{4,r})\,\mathbf{D}\\
\Lambda_{31} &= \operatorname{diag}(c_{2,r})\,\mathbf{D}^2 + \operatorname{diag}(c_{3,r});\\
\Lambda_{32} &= \operatorname{diag}(c_{4,r})\,\mathbf{D};\\
\Lambda_{33} &= \mathbf{D}^2 + \operatorname{diag}(c_{1,r})\,\mathbf{D}
\end{aligned}
\tag{31}
$$

$F_{r+1} = [f_{r+1,0}, f_{r+1,1}, - - -, f_{r+1,N}]^T$, $\Theta_{r+1} = [\theta_{r+1,0}, \theta_{r+1,1}, - - -, \theta_{r+1,N}]^T$, and $\Phi_{r+1} = [\phi_{r+1,0}, \phi_{r+1,1}, - - -, \phi_{r+1,N},]^T$ are vectors of sizes $(N_x + 1) \times 1$, diag$(\cdots)$ represents a diagonal matrix of vectors, and $\mathbf{O}$ is a zero vectors of size $(N_x + 1) \times (N_x + 1)$.

The suitable initial approximations that satisfy the governing boundary conditions of the boundary layer equations (13)-(17) are

$$
\begin{aligned}
f_0(\eta) &= \eta - 1 + e^{-\eta},\\
f_0'(\eta) &= 1 - e^{-\eta}\\
\theta_0(\eta) &= \phi_0(\eta) = e^{-\eta}
\end{aligned}
\tag{32}
$$

4. Results and Discussion

Numerical solutions are obtained using SQLM for the velocity, temperature, and concentration profiles across the boundary layer for different values of the governing parameters. The number of collocation points in the space x variable used to generate the results is $N_x = 40$ in all cases. To ensure the numerical accuracy of the numerical method used, the skin friction coefficient $-f''(0)$ and local Nusselt number $-\theta'(0)$ have been calculated for different values of Falkner-Skan power-law parameter m. From Table 1, it is observed that the data produced by the SQLM code and those reported by Ashwini and Eswara [20], Watanaba [21], and Ullah et al. [22] are excellent agreement. Thus, we are very much confident that the present results are accurate.

Table 2 illustrates the influence of nondimensional governing parameters on the skin friction coefficient, local Nusselt, and local Sherwood numbers. The skin friction coefficient enhances with increase in pressure gradient, permeability, and magnetic parameter. The local Nusselt number is a decreasing function and a local Sherwood number is an increasing function of the pressure gradient parameter, magnetic parameter, Permeability parameter, Prandtl number, Lewis number, thermophoresis parameter, and Eckert number.

Figure 2(a) shows the variation of velocity profiles for different values of pressure gradient parameter β. It clearly demonstrates that the velocity profile increases with an increase in pressure gradient parameter. Because of the increment of wedge angle, the fluid moves much slower and decreases velocity boundary layer thickness. Figure 2(b) shows the effect of permeability parameter κ on the velocity profile. It is observed that increase in κ leads to increase the velocity of the nanofluid on the porous surface and decrease its boundary layer thickness. It is also noticed that both pressure gradient parameter β and permeability parameter κ have no significant effect on both nanofluid temperature and concentration.

Figures 3(a), 3(b), and 4(a) illustrate the influences of magnetic parameter M on the velocity, temperature, and concentration profiles, respectively. Figure 3(a) reveals that the velocity boundary layer thickness decreases with an increase in magnetic parameter. This is due to the fact that the presence of transverse magnetic field sets in Lorentz force, which results in retarding force on the velocity field. Consequently, as the values of magnetic parameter increase, so does the retarding force and hence the velocity profile increase. Figure 3(b) shows that the thermal boundary layer thickness decreases with an increase in magnetic parameter. This is due to additional work expended in dragging the fluid in the boundary layer against the action of the Lorentz force and energy is dissipated as thermal energy which heats the fluid. This reduces the temperature. It is also observed that the concentration profile and its boundary layer thickness decrease with an increase in magnetic parameter as shown in Figure 4(a). Figure 4(b) descries the concentration profile for different values of Lewis number Le. It is clearly observed that the concentration profile and its boundary layer thickness reduce considerably as the Lewis number increases.

The effect of the Prandtl number on the temperature and concentration is shown in Figures 5(a) and 5(b), respectively. It is depicted that the temperature and concentration profiles and their boundary layer thickness reduce significantly as the Prandtl number increase. Because increasing the Prandtl number tends to reduce the thermal diffusivity of the fluid and causes weak penetration of heat inside the fluid. However, in the region near to the boundary surface, the heat transfer rate increases with an increase in Pr. This is due to the fact that the temperature gradient at the surface increase.

The effect of viscous dissipation parameter Ec on the temperature and concentration profiles is presented in Figures 6(a) and 6(b), respectively. The Eckert number expresses the conversion of kinetic energy into internal energy by work done against the viscous fluid stress. It is observed that the temperature increases significantly from the surface and attains a peak value around $\eta = 0.5$ and then decreases in the rest of the region as given in Figure 6(a). This implies that the thermal boundary layer becomes thicker with large Eckert number. The concentration profile gradually reduces near the

Table 1: Comparison of the SQLM results of skin friction coefficient $-f''(0)$ and local Nusselt number $-\theta'(0)$ for various values of m for the case of $\kappa = 0$, M=0, Ec=0, Pr=0.73, Nb=10^{-5}, Nt=0, and Le=0.

	$-f''(0)$				$-\theta'(0)$	
m	Present	Ashwini [20]	Watanaba [21]	Ullah [22]	Present	Watanaba [21]
0.0000	0.46960	0.4696	0.46960	0.4696	0.42016	0.42015
0.0141	0.50461	0.5046	0.50461	0.5046	0.42578	0.42578
0.0435	0.56898	0.5690	0.56898	0.5690	0.43548	0.43548
0.0909	0.65498	0.6550	0.65498	0.6550	0.44730	0.44730
0.1429	0.73200	0.7320	0.73200	0.7320	0.45694	0.45693
0.2000	0.80213	0.8021	0.80213	0.8021	0.46503	0.46503
0.3333	0.92765	0.9277	0.92765	0.9277	0.47814	0.47814
1.0000	1.23258	1.2326		1.2326		

Table 2: Computations of the skin friction coefficient $-f''(0)$, local Nusselt number $-\theta'(0)$ and local Sherwood number $-\phi'(0)$ for various parameters.

β	M	κ	Pr	Ec	Nb	Nt	Le	$-f''(0)$	$-\theta'(0)$	$-\phi'(0)$
0.25	2.0	0.5	0.5	0.5	0.4	0.2	1.5	1.64283184	0.20409760	0.56485047
0.5								1.64925659	0.20245352	0.56792266
1.0								1.66202020	0.19918041	0.57392554
0.25	1.0							1.35213817	0.22650827	0.52246831
	3.0							1.88981423	0.18295134	0.60015609
	5.0							2.30622396	0.14414670	0.65848609
	2.0	0.2						1.56122953	0.21069258	0.55304965
		0.5						1.64283184	0.20409760	0.56485047
		0.8						1.72061427	0.19761936	0.57603379
		0.5	0.1					1.64283184	0.24670503	0.31761537
			0.5					1.64283184	0.20409760	0.56485047
			1.0					1.64283184	0.09226748	0.81573784
			0.5	0.1				1.64283184	0.35278900	0.49744039
				0.5				1.64283184	0.20409760	0.56485047
				1.0				1.64283184	0.01794788	0.64924507
				0.5	0.2			1.64283184	0.22555655	0.58070313
					0.4			1.64283184	0.20409760	0.56485047
					0.8			1.64283184	0.16405080	0.55624299
					0.4	0.1		1.64283184	0.21129537	0.54685694
						0.2		1.64283184	0.20409760	0.56485047
						0.4		1.64283184	0.19012517	0.60871601
						0.2	1.0	1.64283184	0.20846325	0.47924548
							1.5	1.64283184	0.20409760	0.56485047
							2.0	1.64283184	0.20105976	0.63575168

surface up to $\eta = 1$ and then it increases with an increase in the viscous dissipation parameter Ec as highlighted in Figure 6(b).

The influence of the Brownian motion parameter Nb on the nanofluid temperature and concentration profiles is presented in Figures 7(a) and 7(b), respectively. Figure 7(a) reveals that the temperature profile increases with an increase in Nb, particularly in the region close to the surface. The physics behind this phenomenon is that the increased Nb increases the thickness of thermal boundary layer, which finally enhances the temperature. Figure 7(b) remarks that an increase in the values of Nb tends to decrease the concentration profile near the surface. Figures 8(a) and 8(b), respectively, reveal the usual temperature and concentration profiles for various values of thermophoresis parameter Nt. The thermophoresis force generated by the temperature gradient produces a fast flow and more fluid is heated away from the surface. Consequently, the higher the value of Nt increase temperature profile and its boundary layer thickness as given in Figure 8(a). Figure 8(b) reveals that concentration

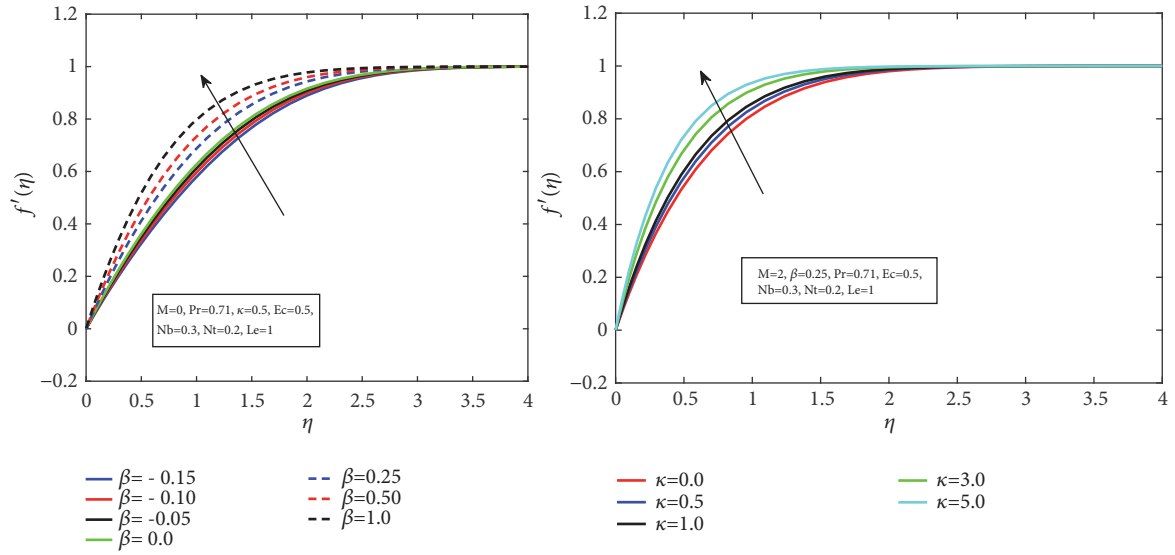

FIGURE 2: (a) Velocity profiles for various values of β. (b) Velocity profiles for various values of κ.

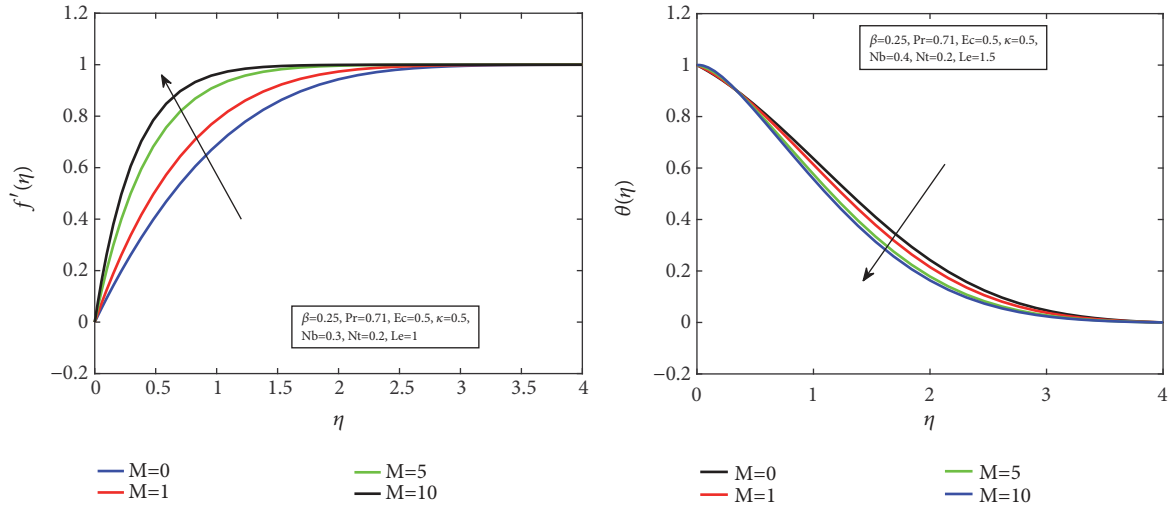

FIGURE 3: (a) Velocity profiles for various values of M. (b) Temperature profiles for various values of M.

profile declines near the boundary surface until $\eta = 0.5$ and afterward it increases with an increase in thermophoresis parameter Nt.

5. Conclusions

The problem of two-dimensional steady laminar MHD boundary layer wedge flow with heat and mass transfer of nanofluid past a porous media with viscous dissipation, Brownian motion, and thermophoresis effects has been studied. Using suitable similarity transformations, the governing equations are transformed to a system of nonlinear ordinary differential equations and solved numerically employing spectral quasilinearization method. From the above discussions the following conclusions are given:

(1) The thickness of velocity boundary layer reduces with an increase in pressure gradient, permeability, and magnetic parameters.

(2) Thermal boundary layer thicker with an increase in Eckert number, Brownian motion, and thermophoresis parameters.

(3) Greater values of Prandtl number, Lewis number, Brownian motion, and magnetic parameter reduce the nanofluid concentration profile.

(4) The skin-friction coefficient at the surface enhances with an increase in pressure gradient, permeability, and magnetic parameters.

(5) The local Nusselt number is a decreasing function, but a local Sherwood number is an increasing function of

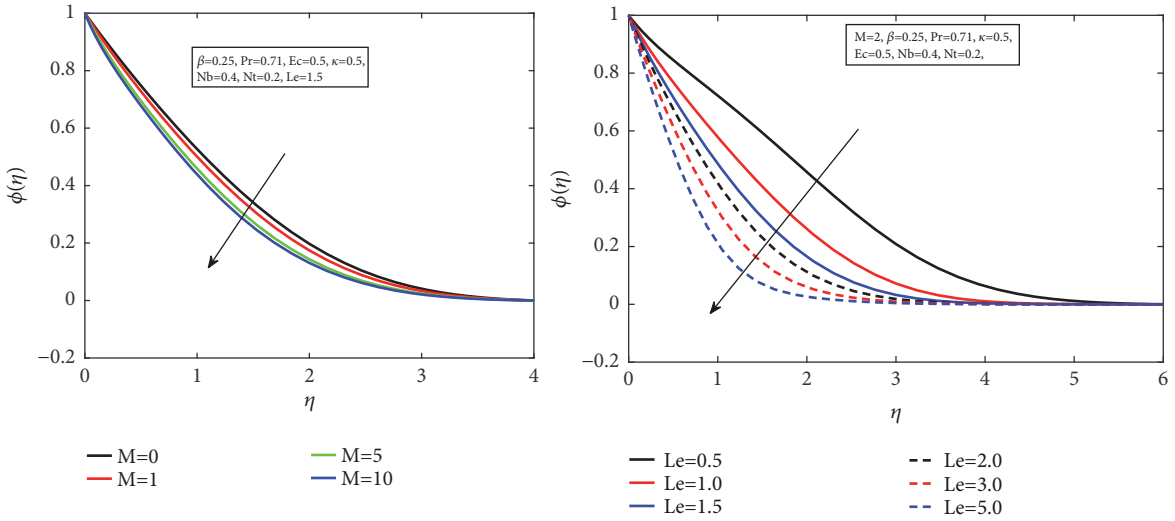

Figure 4: (a) Concentration profiles for various values of M. (b) Concentration profiles for various values of Le.

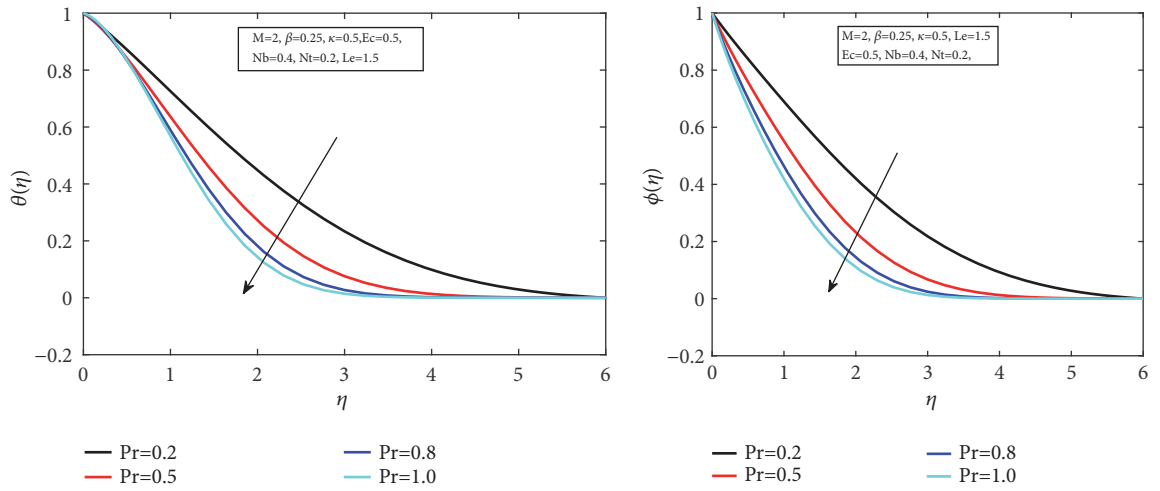

Figure 5: (a) Temperature profiles for various values of Pr. (b) Concentration profiles for various values of Pr.

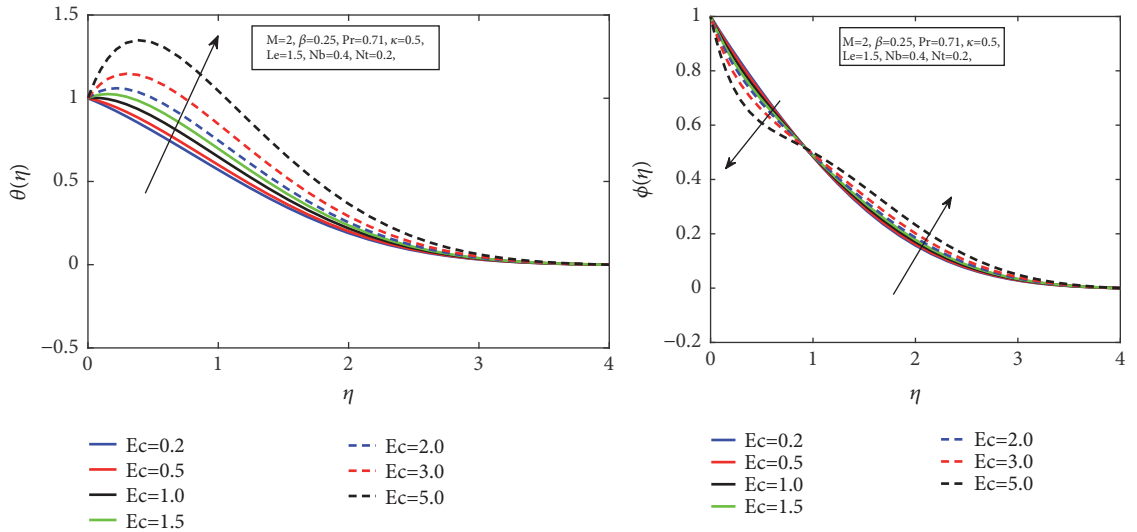

Figure 6: (a) Temperature profiles for various values of Ec. (b) Concentration profiles for various values of Ec.

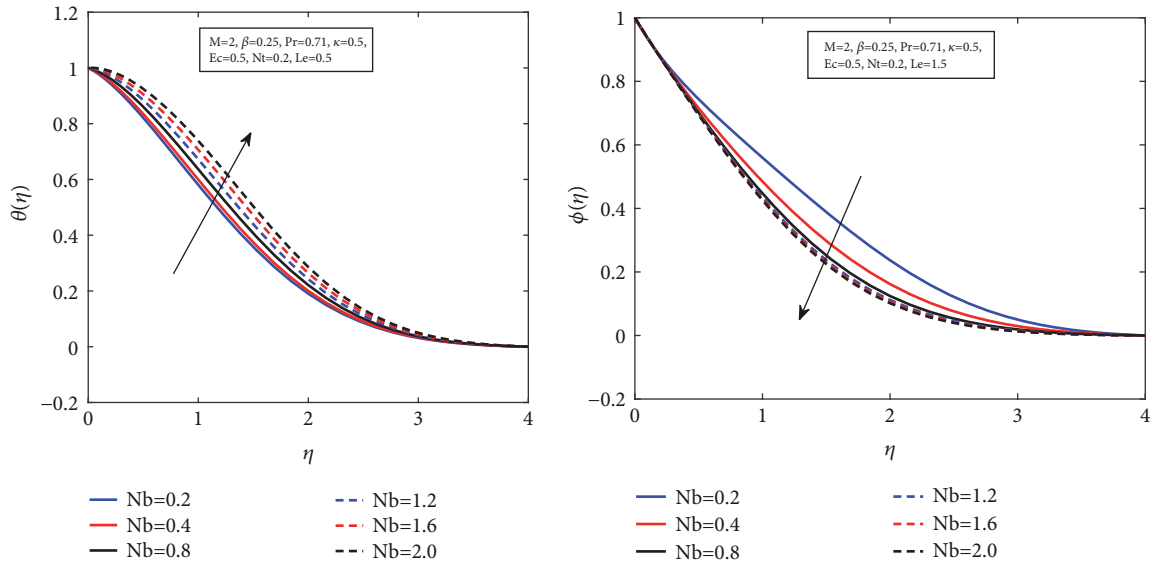

Figure 7: (a) Temperature profiles for various values of Nb. (b) Concentration profiles for various values of Nb.

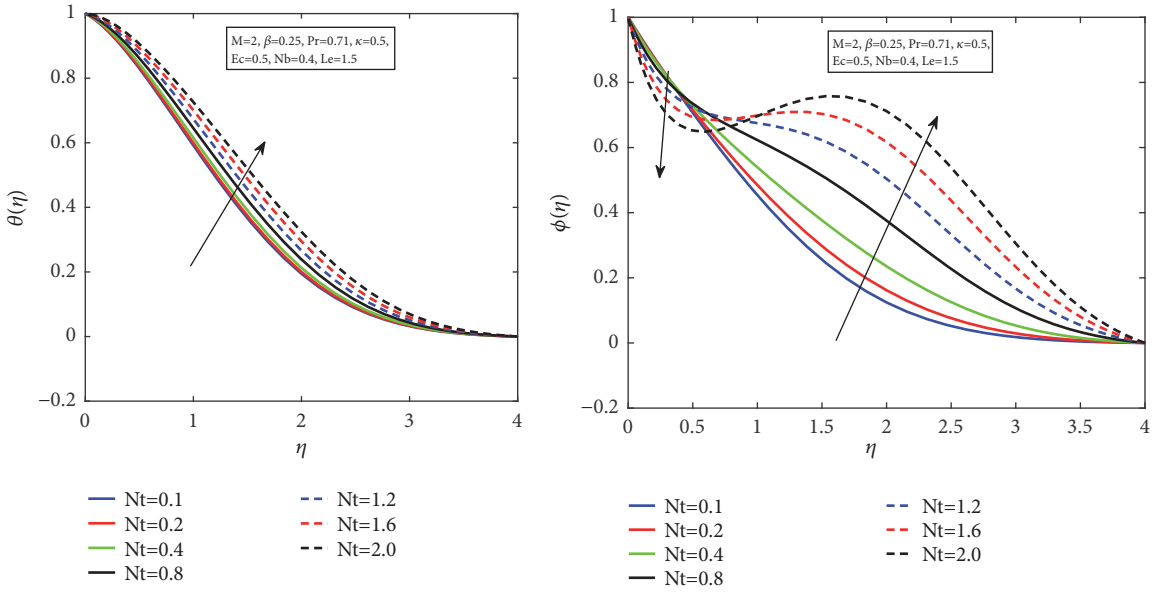

Figure 8: (a) Temperature profiles for various values of Nt. (b) Concentration profiles for various values of Nt.

the pressure gradient parameter, magnetic parameter, permeability parameter, thermophoresis parameter, and Eckert number.

Nomenclature

B_0: Magnetic field strength
C_f: Local Skin friction coefficient
C_p: Specific heat capacity
C_w: Concentration at the surface of the wall
C_∞: Ambient concentration
D: Chebyshev Differentiation matrix
D_B: Brownian diffusion coefficient
D_T: Thermophoresis diffusion coefficient
Ec: Eckert number
f: Dimensionless stream function
J_c: Conduction current
K: Permeability of porous medium
k: Thermal conductivity
L: Characteristic length
Le: Lewis number
M: Magnetic parameter
m: Falkner-Skan power-law parameter
M_w: Wall mass flux
Nb: Brownian motion parameter
Nt: Thermophoresis parameter
Nu_x: Local Nusselt number
Pr: Prandtl number

q_w: Wall heat flux
Re_x: Local Reynolds number
S_φ: General source term
Sh_x: Local Sherwood number
T_∞: Ambient temperature
U: Inviscid velocity at the wedge
U_∞: Free stream velocity
u: Fluid velocity in the x direction
v: Fluid velocity in the y direction

Greek Symbols

α: Thermal diffusivity
β: Pressure gradient parameter
Γ: General diffusion coefficient
η: Dimensionless similarity variable
θ: Dimensionless temperature
κ: Permeability parameter
μ_f: Dynamic viscosity of the base fluid
ν_f: Kinematic viscosity of the base fluid
ρ_f: Density of the base fluid
σ: Electrical conductivity
τ: Ratio of effective heat capacity of nanoparticle and heat capacity of base fluid
τ_w: Wall shear stress
ϕ: Dimensionless concentration
ψ: Stream function
φ: General scalar variable

Subscripts

∞: Condition at the free stream
w: Condition at the surface.

Data Availability

The data used to support the findings of this study are available from the corresponding author upon request.

Conflicts of Interest

The authors declare that they have no conflicts of interest.

References

[1] V. Nagendramma, K. Sreelakshmi, and G. Sarojamma, "MHD heat and mass transfer flow over a stretching wedge with convective boundary condition and thermophoresis," *Science Direct, Procedia Engineering*, vol. 127, pp. 963–969, 2015.

[2] V. M. Falkner and S. W. Skan, "Some approximate solutions of the boundary layer equations," *Philosophical Magazine*, vol. 12, pp. 865–896, 1931.

[3] D. R. Hartree, "On an equation occurring in Falkner and Skan's approximate treatment of the equations of the boundary layer," *Mathematical Proceedings of the Cambridge Philosophical Society*, vol. 33, no. 2, pp. 223–239, 1937.

[4] E. R. G. Eckert, "Die berechnungs/des warmeuberganges in der laminaren grenzschicht um stomter korper," *VDI-Forschungsheft*, vol. 416, pp. 1–24, 1942.

[5] M. J. Martin and I. D. Boyd, "Falkner-Skan flow over a wedge with slip boundary conditions," *Journal of Thermophysics and Heat Transfer*, vol. 24, no. 2, pp. 263–270, 2010.

[6] M. A. Sattar, "A local similarity transformation for the unsteady two-dimensional hydrodynamic boundary layer equations of a flow past awedge," *International Journal of Applied Mathematics and Mechnics*, vol. 7, no. 1, pp. 15–28, 2011.

[7] R. Kandasamy, I. Muhaimin, A. B. Khamis, and R. B. Roslan, "Unsteady Hiemenz flow of Cu-nanofluid over a porous wedge in the presence of thermal stratification due to solar energy radiation: Lie group transformation," *International Journal of Thermal Sciences*, vol. 65, pp. 196–205, 2013.

[8] M. Turkyilmazoglu, "Slip flow and heat transfer over a specific wedge: an exactly solvable Falkner-Skan equation," *Journal of Engineering Mathematics*, vol. 92, no. 1, pp. 73–81, 2015.

[9] G. Makanda, *Numerical study of convective fluid flow in porous and non-porous media [Ph.D. thesis]*, University of KwaZulu-Natal, Pietermaritzburg, South Africa, 2015.

[10] S. Abbasbandy, R. Naz, T. Hayat, and A. Alsaedi, "Numerical and analytical solutions for Falken-Skan flow of MHD Maxwell fluid," *Applied Mathematics and Computation*, vol. 242, pp. 569–575, 2014.

[11] N. T. El-Dabe, A. Y. Ghaly, R. R. Rizkallah, K. M. Ewis, and A. S. Al-Bareda, "Numerical solution of MHD boundary layer flow of non-newtonian casson fluid on a moving wedge with heat and mass transfer and induced magnetic field," *Journal of Applied Mathematics and Physics*, vol. 3, no. 6, pp. 649–663, 2015.

[12] M. S. Khan, I. Karim, M. S. Islam, and M. Wahiduzzaman, "MHD boundary layer radiative, heat generating and chemical reacting flow past a wedge moving in a nanofluid," *Nano Convergence*, vol. 1, pp. 20–28, 2014.

[13] D. Srinivasacharya, U. Mendu, and K. Venumadhav, "MHD boundary layer flow of a nanofluid past a wedge," *Science Direct, Procedia Engineering*, vol. 127, pp. 1064–1070, 2015.

[14] H. Rasheed, A. Rehman, N. Sheikh, and S. Iqbal, "MHD boundary layer flow of nanofluid over a continuously moving stretching surface," *Applied and Computational Mathematics*, vol. 6, no. 6, pp. 265–270, 2017.

[15] A. Nageeb, H. Haroun, S. Mondal, and P. Sibanda, "Effects of thermal radiation on mixed convection in a MHD nanofluid flow over a stretching sheet using a spectral relaxation method," *International Journal of Mathematical, Computational, Physical, Electrical and Computer Engineering*, vol. 11, no. 2, 2017.

[16] E. M. Arthur and I. Y. Seini, "Hydromagnetic stagnation point flow over a porous stretching surface in the presence of radiation and viscous dissipation," *Applied and Computational Mathematics*, vol. 3, no. 5, pp. 191–196, 2014.

[17] B. K. Ramesh, R. K. Shreenivas, L. N. Achala, and N. M. Bujurke, "Similarity solutions of the MHD boundary layer flow past a constant wedge within porous media," *Mathematical Problems in Engineering*, vol. 2017, Article ID 1428137, 11 pages, 2017.

[18] E. Haile and B. Shankar, "Boundary-layer flow of nanofluids over a moving surface in the presence of thermal radiation, viscous dissipation and chemical reaction," *Journal of Applied Mathematics*, vol. 10, no. 2, pp. 952–969, 2015.

[19] S. S. Majety and K. Gangadhar, "Viscous dissipation effects on radiative MHD boundary layer flow of nano fluid past a wedge through porous medium with chemical reaction," *IOSR Journal of Mathematics*, vol. 12, no. 5, pp. 71–81, 2016.

[20] G. Ashwini and A. T. Eswara, "MHD Falkner-Skan boundary layer flow with internal heat generation or absorption," *International Journal of Mathematical and Computational Sciences*, vol. 6, no. 5, pp. 556–559, 2012.

[21] T. Watanabe, "Thermal boundary layer over a wedge with uniform suction and injection in forced flow," *Acta Mechanica*, vol. 83, no. 3-4, pp. 119–126, 1990.

[22] I. Ullah, I. Khan, and S. Shafie, "Hydromagnetic Falkner-Skan flow of Casson fluid past a moving wedge with heat transfer," *Alexandria Engineering Journal*, vol. 55, no. 3, pp. 2139–2148, 2016.

[23] S. S. Motsa, P. Sibanda, J. M. Ngnotchouye, and G. T. Marewo, "A spectral relaxation approach for unsteady boundary-layer flow and heat transfer of a nanouid over a permeable stretching/shrinking sheet," *Advances in Mathematical Physics*, vol. 2014, Article ID 564942, 10 pages, 2014.

[24] S. S. Motsa, Z. G. Makukula, and S. Shateyi, "Spectral Local Linearisation Approach for Natural Convection Boundary Layer Flow," *Mathematical Problems in Engineering*, vol. 2013, Article ID 765013, 7 pages, 2013.

[25] V. M. Magagula, S. S. Motsa, P. Sibanda, and P. G. Dlamini, "On a bivariate spectral relaxation method for unsteady magnetohydrodynamic flow in porous media," *SpringerPlus*, vol. 5, article 455, 2016.

[26] S. S. Motsa, "A new spectral relaxation method for similarity variable nonlinear boundary layer flow systems," *Chemical Engineering Communications*, vol. 201, no. 2, pp. 241–256, 2013.

[27] J. Zhou, "The constants in a posteriori error indicator for state-constrained optimal control problems with spectral methods," *Abstract and Applied Analysis*, vol. 2014, Article ID 946026, 8 pages, 2014.

[28] D. Gottlieb and J. S. Hesthaven, "Spectral methods for hyperbolic problems," *Journal of Computational and Applied Mathematics*, vol. 128, pp. 83–131, 2001.

[29] S. S. Motsa, V. M. Magagula, and P. Sibanda, "A bivariate chebyshev spectral collocation quasilinearization method for nonlinear evolution parabolic equations," *The Scientific World Journal*, vol. 2014, Article ID 581987, 13 pages, 2014.

[30] A. Nicholas, *An Introduction to Magnetohydrodynamics*, Battista Stony Brook University, New York, NY, USA, 2010.

[31] H. K. Versteeg and W. Malalasekera, *An Introduction to Computational Fluid Dynamics: The Finite Volume Method*, vol. 24, Pearson Education Limited, Harlow, UK, 2nd edition, 2007.

[32] M. S. Alam, M. Ali, M. A. Alim, M. J. Munshi, and M. Z. Chowdhury, "Solution of Falkner- Skan unsteady MHD boundary layer flow and heat transfer past a moving porous wedge in a nanofluid," *Science Direct Procedia Engineering*, vol. 194, pp. 414–420, 2017.

[33] S. S. Motsa, "A new spectral local linearization method for nonlinear boundary layer flow problems," *Journal of Applied Mathematics*, vol. 2013, Article ID 423628, 15 pages, 2013.

[34] L. N. Trefethen, *Spectra Methods in MATLAB*, Society for Industrial and Applied Mathematics, Philadelphia, PA, USA, 1st edition, 2000.